

MODELLING VALIDATION FOR NLEVM NEEDS EXPERIMENTAL FACILITIES FOR SUPPORTING THE DESIGN OF INNOVATIVE COMPONENTS

Emanuela Colombo, Fabio Inzoli, Riccardo Mereu

Politecnico di Milano, Department of Energy, Piazza Leonardo da Vinci, 32 - 20133 MILANO

PURPOSE

The study is focused on an application of a two equation turbulence model based on Reynolds non linear eddy viscosity approximation (NLEVM) implemented by the author in a commercial code and here improved. This research area is finally devoted to obtain useful and interesting results for increasing the accuracy of CFD prediction when applied to complex flow and industrial geometry.

The model is a second order $k-\epsilon$ model based over Shih, Zhu and Lumley (1993) and Craft, Launder and Suga (1996) and it is implemented in the finite volume commercial code ANSYS-FLUENT v. 6.3.26 through specific additional subroutines.

TURBULENCE MODELLING AND IMPROVEMENT

The Non Linear Eddy Viscosity Model (NLEVM) formulation proposed in the past work was already characterized by a realizable formulation of the turbulent viscosity where C_μ has the same structure proposed by Shih, Zhu, Lumley and modified in according to experimental value obtained by an experimental campaign done at the THTLab of the University of Tokyo:

$$C_\mu = \frac{2/3}{\mu} \frac{1}{3.9+S} \quad (1)$$

where $S = \frac{k}{\epsilon} \sqrt{\frac{1}{2} S_{ij} S_{ij}}$ represents the mean strain rate invariant.

Furthermore a second order correlation between the Reynolds stress tensor and the mean strain rate tensor was proposed:

$$-\rho \overline{u_i u_j} = \frac{2}{3} \rho k \delta_{ij} + \mu_t S_{ij} - C_1 \mu_t \frac{k}{\epsilon} \left[S_{ik} S_{kj} - \frac{1}{3} \delta_{ij} S_{kl} S_{kl} \right] - C_2 \mu_t \frac{k}{\epsilon} \left[\Omega_{ik} S_{kj} + \Omega_{jk} S_{ki} \right] + C_3 \mu_t \frac{k}{\epsilon} \left[\Omega_{ik} \Omega_{kj} - \frac{1}{3} \delta_{ij} \Omega_{kl} \Omega_{kl} \right] \quad (2)$$

where $S_{ij} = \left(\frac{\partial U_i}{\partial x_j} + \frac{\partial U_j}{\partial x_i} \right)$, $\Omega_{ij} = \left(\frac{\partial U_i}{\partial x_j} - \frac{\partial U_j}{\partial x_i} \right)$ and $C_1 = \frac{0.8/C_\mu}{1000+S^3}$, $C_2 = \frac{11/C_\mu}{1000+S^3}$, $C_3 = \frac{4.5/C_\mu}{1000+S^3}$

In the present study a damping function is added to the turbulent viscosity formulation. The formulation is defined by the Prandtl-Kolmogorov relation:

$$\mu_t = \rho C_\mu \frac{k^2}{\epsilon} f \quad \text{where} \quad f = \frac{0.024 + \frac{Re_\tau}{6}}{1 + \frac{Re_\tau}{6}} \quad (3)$$

represents the damping function for the turbulent viscosity proposed by Wilcox.

In the test cases and industrial application presented the wall region has been resolved using the approach of Enhanced Wall Treatment natively implemented in the code.

Model's improvement validation

The proposed model, 2ordke and its improvement, 2ordkelr, are compared with the linear native model of the code (realizable $k-\epsilon$, rke, and RNG $k-\epsilon$, RNGke) and with experimental data, exp.

The validation with the Square Duct is referred to experimental data of Cheesewright et al.. The Reynolds number based on the mean velocity flow U_b (centerline velocity) and on the half height of the duct h is $Re_b = 4410$. The domain is characterized by periodic conditions. Fig. 1 (right) shows the presence of the secondary flows with a magnitude roughly about 1.2% of the streamwise velocity (U_b). In Fig. 1 (left) the dimensionless span velocity profile in the cross section plane along a line close to the wall ($x/h=0.16$) is shown.

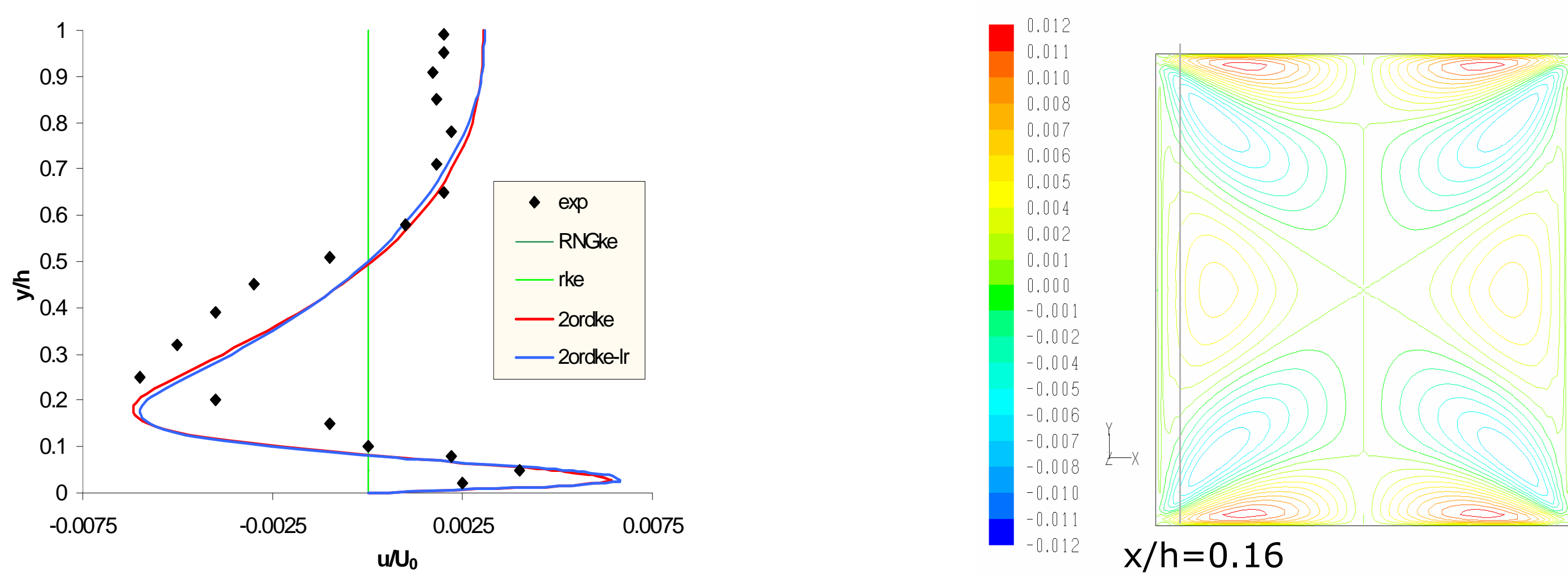


Fig. 1 (left) Dimensionless velocity profile along a line ($x/h=0.16$); (right) Contours of the dimensionless velocity (x component) orthogonal to the flow field direction (z direction)

For the Backward Facing Step experimental data are taken from Jovic and Driver already used by Moin et al. in order to validate their DNS simulation. The geometry is characterized by a double expansion duct, with an expansion ratio equal to 1.2. The Reynolds number, based on the height of the step $h=0.96$ cm and the free stream velocity $U_0=7.72$ m/s measured 3 cm upstream the step, is $Re_h=5100$. In Fig. 2 the pressure coefficient is evaluated, whereas in Tab. 1 the reattachment point calculated is compared with experimental data.

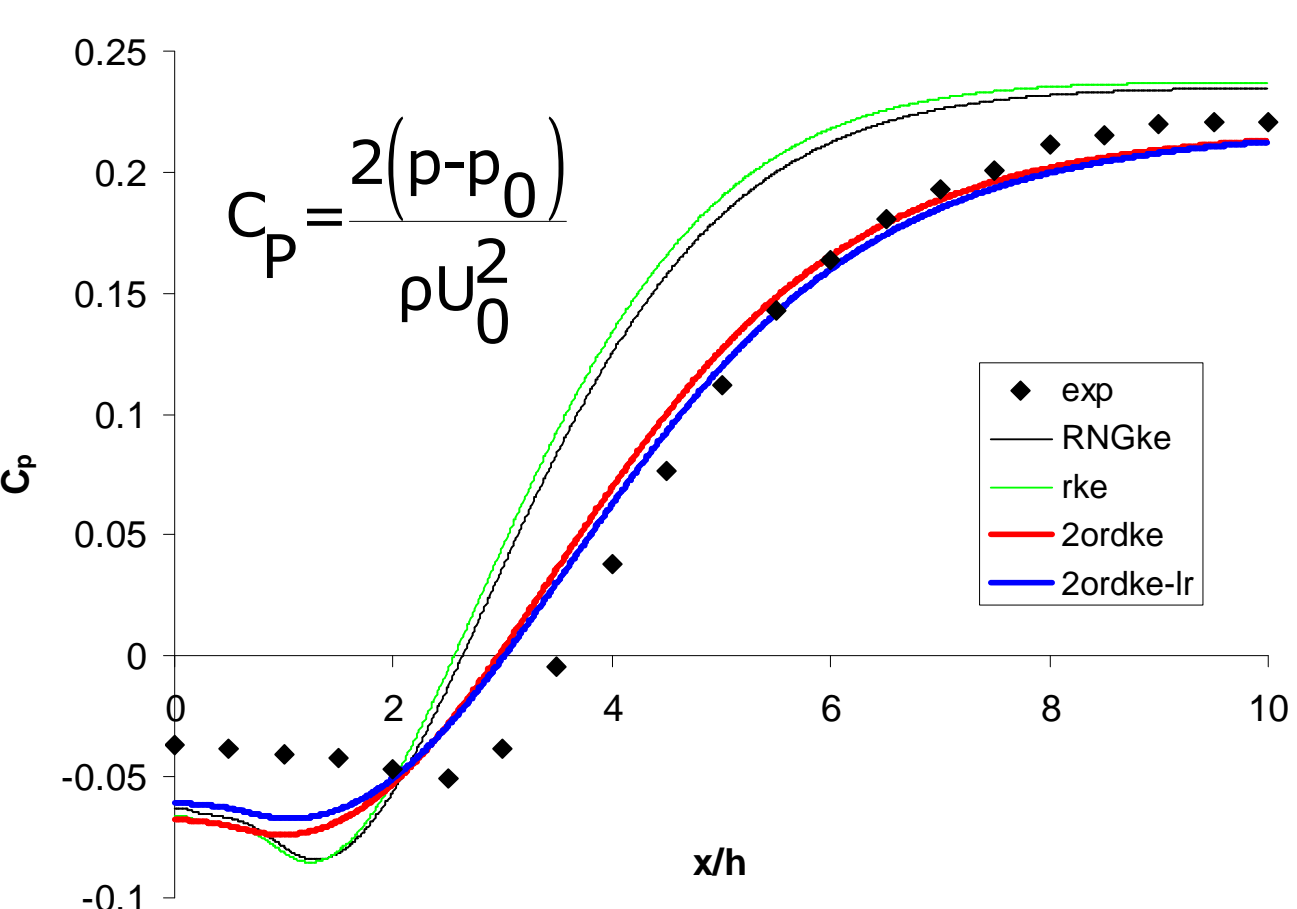


Fig. 2 Pressure Coefficient C_p

Models	Reattachment	Error (%)
Rke	5.6 h	-8.2
RNGke	5.8 h	-4.9
2ordke	5.6 h	-8.2
2ordkelr	5.9 h	-3.3
Exp. data	6.1 h	

Tab. 1 Reattachment point

The IRIS REACTOR

IRIS is a novel light water reactor with a modular, integral primary system configuration with the concept pursued by an international group. IRIS is designed to satisfy four key requirements: enhanced safety, improved economics, proliferation resistance and waste minimization. Its main features are: medium power (up to 335 MWe/module); a simplified compact design where the primary vessel houses steam generators, pressurizer and pumps; a novel, extremely effective safety approach; and, optimized maintenance with intervals of at least four years.

The CFD Group has been established at the beginning of 2004 with the mission of:

- investigating the requirements for CFD application in the nuclear field
- identifying specific applications for IRIS and verify the benefits that the IRIS project may gain from CFD
- setting up an international framework for promoting joint CFD projects and researches

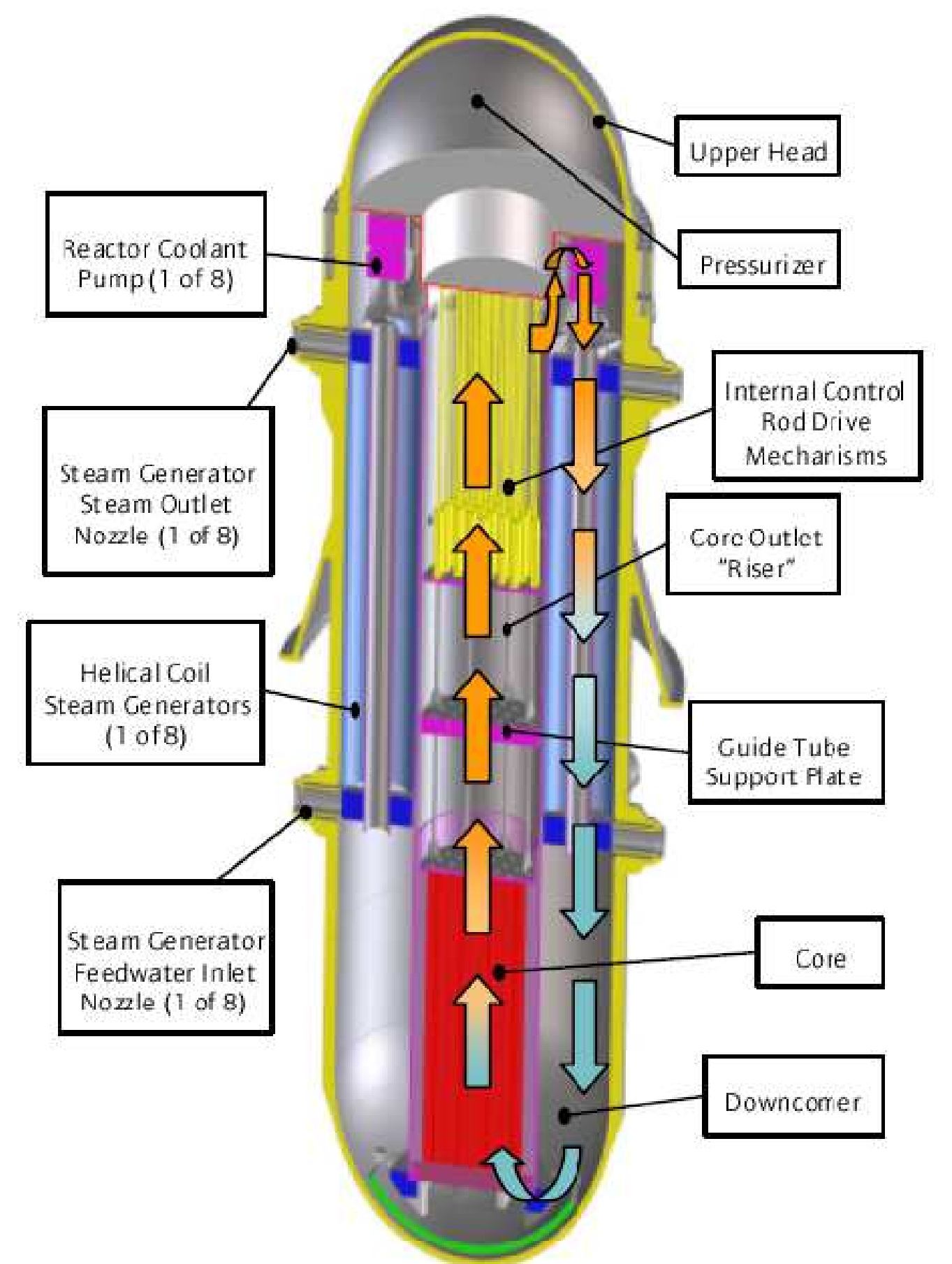


Fig. 3 Layout of the IRIS reactor

No experimental data are available for the IRIS reactor, since no one of the facilities due to be built for the licensing is still operating.

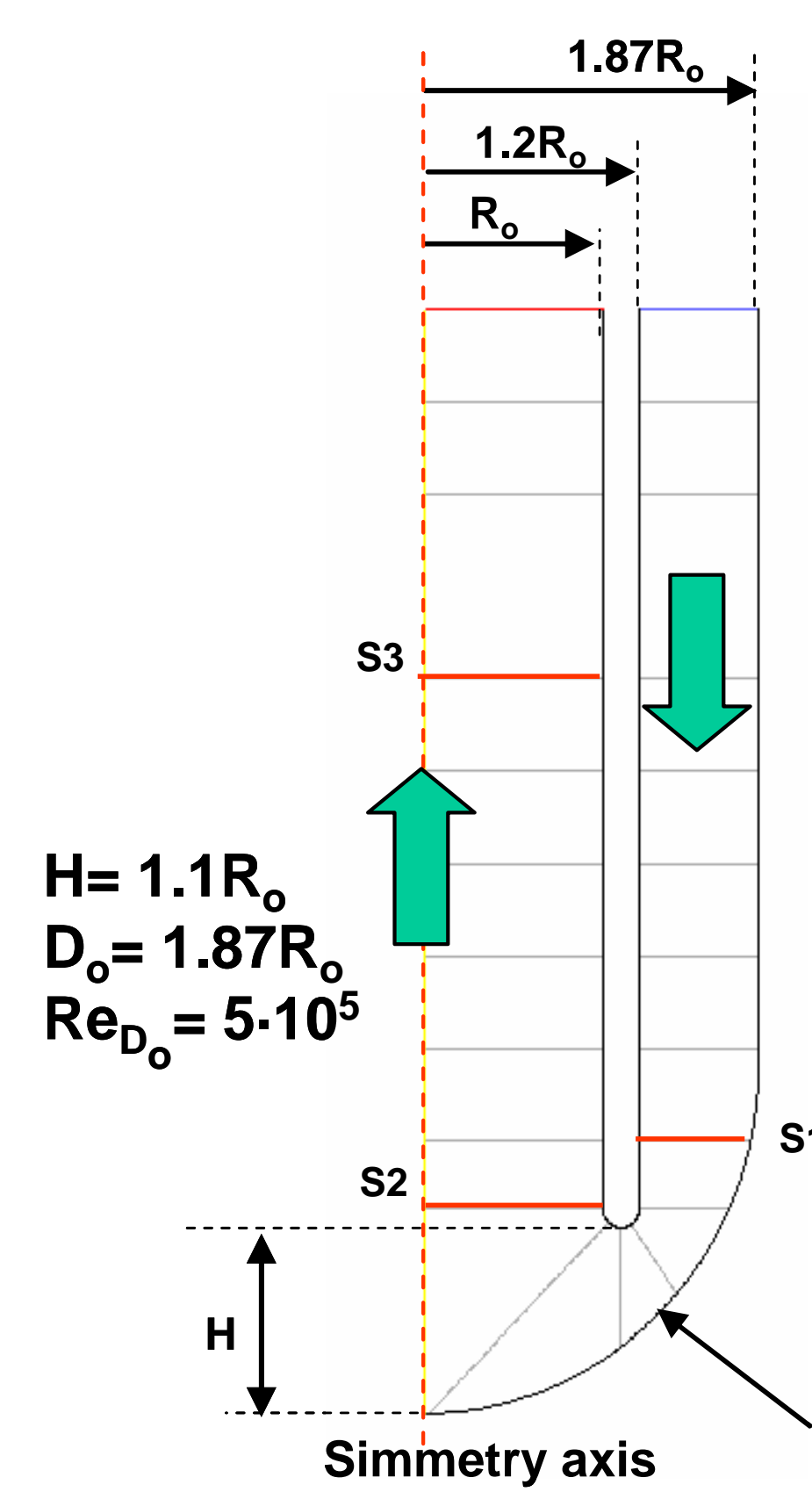


Fig. 4 Domain of the IRIS downcomer

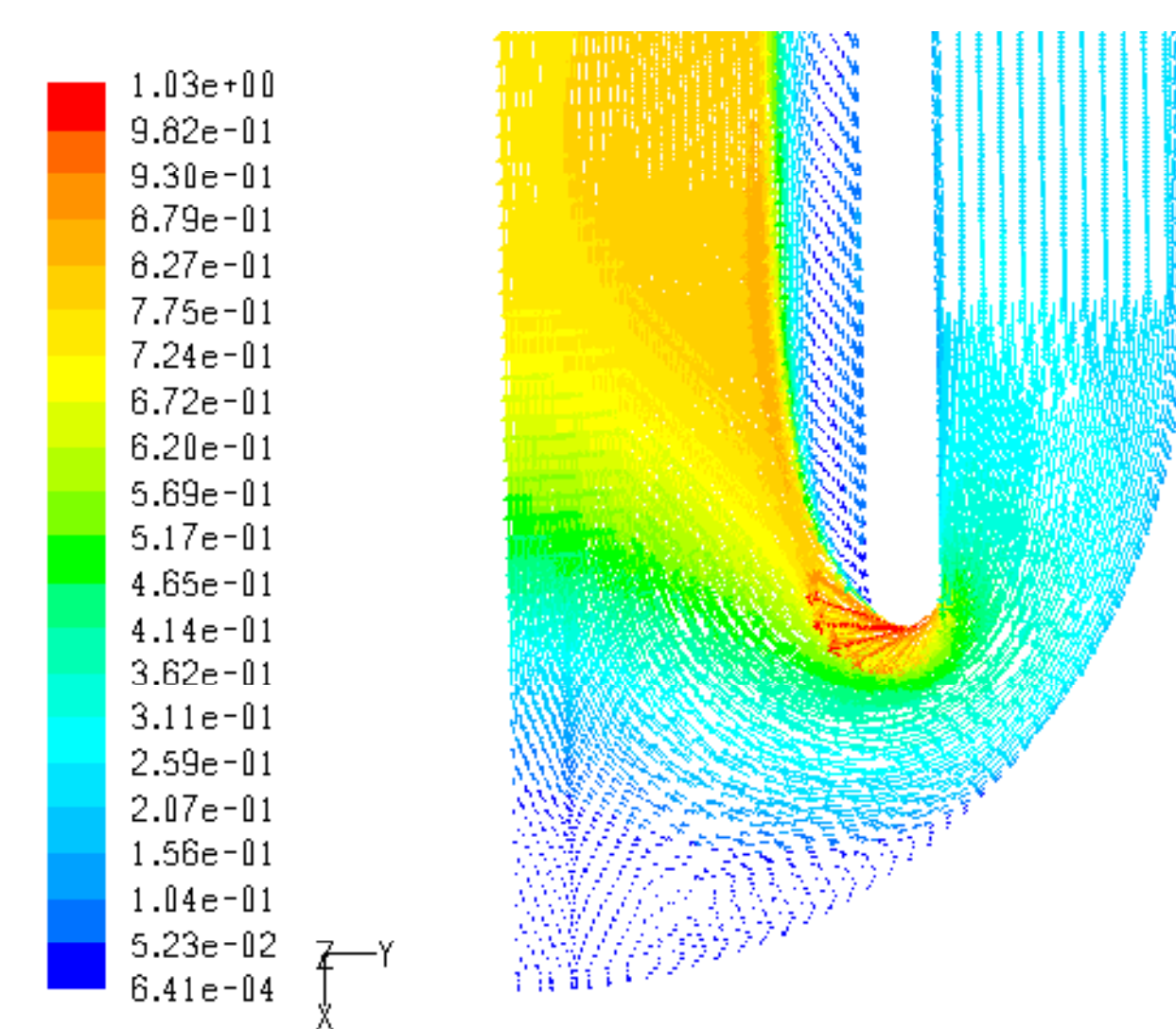


Fig. 6 Vector of velocity magnitude

The geometry used for such application (Fig. 4) is similar to that of the IRIS downcomer lower plenum (a tube bend with contraction and expansion area) and therefore presents characteristics which a linear relationship between strain and stress can not correctly simulate. The Reynolds number based on internal flow model diameter D_0 is equal to $5 \cdot 10^5$.

In Fig. 5 a-c the differences obtained comparing different models are more relevant where results are sensitive to curvature effects. Indeed, Fig. 5a shows the axial velocity before the bend and no significant differences may be underlined between linear and second order models while Fig. 5b, taken just after the bend as well as Fig. 5c, taken in the region where the flow is still developing, show relevant differences.

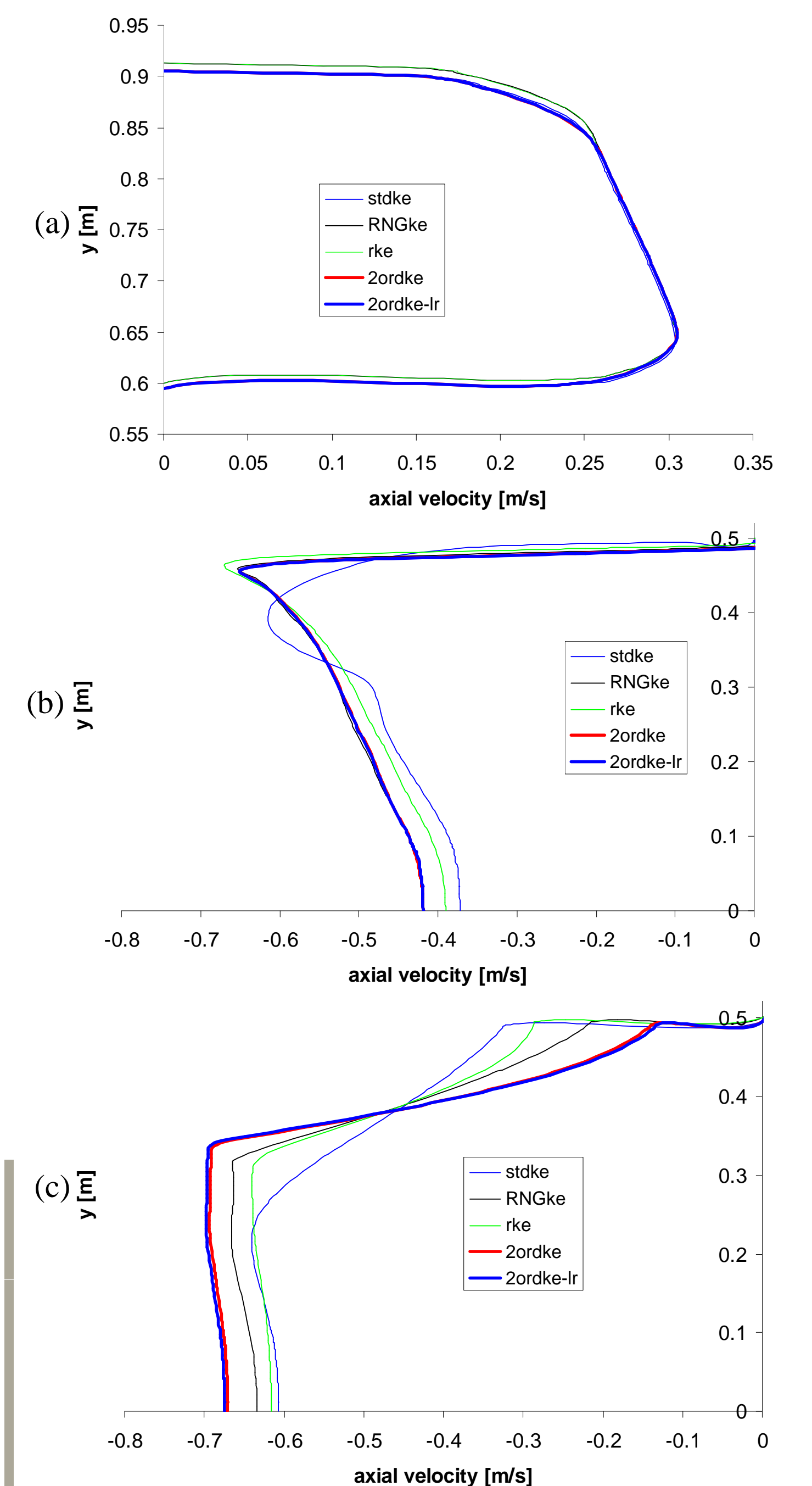


Fig. 5 Axial Velocity along: (a) line "S1" at $1.5R_0$, (b) line "S2" at $1.2R_0$, (c) line "S3" at $4R_0$ from the downcomer lower apex

Models	Reattachment (m)	Dimensionless Reattachment
stdke	0.077	$0.154R_0$
RNGke	0.857	$1.714R_0$
rke	0.387	$0.774R_0$
2ordke	0.977	$1.954R_0$
2ordkelr	1.007	$2.014R_0$

Tab. 2 Reattachment point

CONCLUSION

By means of a comparison with standard $k-\epsilon$, RNG- $k-\epsilon$ and Realizable- $k-\epsilon$, natively implemented in the commercial CFD code used, it is possible to capture the distinguished figures associated with the non linear dependency of the stress-strain relationship. This is also evident in the case study of the IRIS-like geometry which open further opportunity of application for the implemented model.

Final evaluation of the implemented model accuracy would require experimental data on the IRIS-like geometry. Indeed, it is worthy to note that the consortium is nowadays working for preparing an experimental facility in order to set up a numerical and experimental system that can support the design and the licensing of the reactor.